

1 **Norilskite, (Pd,Ag)<sub>7</sub>Pb<sub>4</sub>, a new mineral from Noril'sk -Talnakh deposit, Russia**

2  
3 A. VYMAZALOVÁ<sup>1\*</sup>, F. LAUFEK<sup>1</sup>, S.F. SLUZHENIKIN<sup>2</sup>, C.J. STANLEY<sup>3</sup>

4  
5 <sup>1</sup>Czech Geological Survey, Geologická 6, 152 00 Prague 5, Czech Republic

6 \*E-mail: [anna.vymazalova@geology.cz](mailto:anna.vymazalova@geology.cz)

7  
8 <sup>2</sup>Institute of Geology of Ore Deposits, Petrology, Mineralogy and Geochemistry Russian  
9 Academy of Sciences, Staromonetnyi per. 35, Moscow 119017, Russia

10  
11 <sup>3</sup>Department of Earth Sciences, Natural History Museum, London SW7 5BD, UK

12  
13  
14 **ABSTRACT**

15 Norilskite, (Pd,Ag)<sub>7</sub>Pb<sub>4</sub> is a new platinum-group mineral discovered in the Mayak mine of the  
16 Talnakh deposit, Russia. It forms anhedral grains in aggregates (up to about 400 μm) with  
17 polarite, zvyagintsevite, Pd-rich tetra-auricupride, Pd-Pt bearing auricupride, Ag-Au alloys,  
18 (Pb,As,Sb) bearing atokite, mayakite, Bi-Pb rich kotulskite and sperrylite in pentlandite,  
19 cubanite and talnakhite. Norilskite is brittle, has a metallic lustre and a grey streak. Values of  
20 VHN<sub>20</sub> fall between 296 and 342 kg/mm<sup>2</sup>, with a mean value of 310 kg/mm<sup>2</sup>, corresponding  
21 to a Mohs hardness of approximately 4. In plane-polarized light, norilskite is orange-brownish  
22 pink, has moderate to strong bireflectance, orange-pink to greyish-pink pleochroism, and  
23 strong anisotropy; it exhibits no internal reflections. Reflectance values of norilskite in air (R<sub>o</sub>,  
24 R<sub>e</sub>, in %) are: 51.1, 48.8 at 470nm, 56.8, 52.2 at 546nm, 59.9, 53.5 at 589nm and 64.7, 55.5 at  
25 650nm. Sixteen electron-microprobe analyses of natural norilskite gave an average

26 composition: Pd 44.33, Ag 2.68, Bi 0.33, and Pb 52.34, total 99.68 wt.%, corresponding to the  
27 empirical formula  $(\text{Pd}_{6.56}\text{Ag}_{0.39})_{\Sigma 6.95}(\text{Pb}_{3.97}\text{Bi}_{0.03})_{\Sigma 4.00}$  based on 4 Pb+Bi atoms; the average of  
28 eight analyses on synthetic norilskite is: Pd 42.95, Ag 3.87, and Pb 53.51, total 100.33 wt.%,  
29 corresponding to  $(\text{Pd}_{6.25}\text{Ag}_{0.56})_{\Sigma 6.81}\text{Pb}_{4.00}$ . The mineral is trigonal, space group  $P3_121$ , with  $a$   
30  $8.9656(4)$ ,  $c$   $17.2801(8)$  Å,  $V$   $1202.92(9)$  Å<sup>3</sup> and  $Z = 6$ . The crystal structure was solved and  
31 refined from the powder X-ray-diffraction data of synthetic  $(\text{Pd,Ag})_7\text{Pb}_4$ . Norilskite  
32 crystallizes in the  $\text{Ni}_{13}\text{Ga}_3\text{Ge}_6$  structure type, related to nickeline. The strongest lines in the X-  
33 ray powder diffraction pattern of synthetic norilskite [ $d$  in Å ( $I$ ) ( $hkl$ ) ] are:  
34  $3.2201(29)(023,203)$ ,  $2.3130(91)(026,206)$ ,  $2.2414(100)(220)$ ,  $1.6098(28)(046,406)$ ,  
35  $1.3076(38)(246,462)$ ,  $1.2942(18)(600)$ ,  $1.2115(37)(22.12,12.13)$ ,  $0.9626(44)(06.12,60.12)$ .  
36 The mineral is named for the locality, the Noril'sk district in Russia.

37

38

39 **Keywords:** norilskite, platinum-group mineral,  $(\text{Pd,Ag})_7\text{Pb}_4$  phase, electron-microprobe data,  
40 reflectance data, X-ray-diffraction data, crystal structure, Mayak mine, Talnakh deposit,  
41 Noril'sk district, Russia.

42

43

44

45

46

47

48

49

50

51 **Introduction**

52

53 The holotype specimen (polished section), that contains norilskite, ideally  $(\text{Pd,Ag})_7\text{Pb}_4$ , comes  
54 from the massive pentlandite-cubanite-talnakhite ore from the Mayak mine in the Talnakh  
55 deposit of the Noril'sk district, Russia. The sample was found at coordinates:  $69^\circ 30' 20''$  N  
56 and  $88^\circ 27' 17''$  E. The phase with the corresponding chemical composition, described as  
57 unnamed  $(\text{Pd,Ag})_2\text{Pb}$ , has been also observed in the massive pentlandite-cubanite-talnakhite  
58 ore in Komsomolsky mine of the Talnakh deposit and in the massive pentlandite-talnakhite  
59 ore in Zapolyarny (Trans-Polar) mine of the Noril'sk I deposit (Sluzhenikin and Mokhov,  
60 2015). Norilskite formed in post magmatic conditions, with decreasing temperature  
61 (Sluzhenikin and Mokhov, 2015), most likely below  $400^\circ\text{C}$ .

62 The ore deposits of the Noril'sk-Talnakh district are associated with hypabyssal  
63 intrusions related to the Siberian flood basalt province. Different types of ore can be  
64 distinguished in terms of sulphide content, metal proportions and position within the host  
65 intrusion. Extensive studies have been dedicated to Noril'sk ores and deposits (e.g. Genkin *et al.*,  
66 1981, Distler *et al.*, 1988, Naldrett *et al.*, 1992, Czamanske *et al.*, 1992, Komarova *et al.*,  
67 2002, Sluzhinikin, 2011, Sluzhinikin and Mohkov, 2015, among others).

68 Almost half of all known named platinum-group minerals were reported from the Noril'sk  
69 ores, and also a number of unidentified phases. Furthermore, around 17 new platinum-group  
70 minerals, among other minerals, were discovered from the Noril'sk deposits.

71

72 **Mineral name and type material**

73

74 Both mineral and name were approved by the Commission on New Minerals, Nomenclature  
75 and Classification of the International Mineralogical Association (IMA No 2015-008). The

76 mineral is named for the locality, the Noril'sk district, Russia. The mineral name norilskite  
77 was proposed for an alloy of Pt-Pd-Fe-Ni-Cu found in places near the Noril'sk deposits by  
78 Zviaginцев (1940). Nevertheless, Genkin (1968) proved that it was a mixture of several PGE  
79 minerals. Since that time no mineral species with the name norilskite was proposed.

80 The holotype (polished section) is deposited at the Department of Earth Sciences of the  
81 Natural History Museum, London, UK, catalogue No BM 2015, 1 and co-type material  
82 (polished section) is deposited in the Fersman Mineralogical Museum, Moscow, Russia,  
83 catalogue No 4694/1.

84

#### 85 **Appearance, physical and optical properties**

86

87 Norilskite forms anhedral grains (about 10 to 20  $\mu\text{m}$  in diameter, in case of type material the  
88 grain reaches almost 400  $\mu\text{m}$ ) in aggregates with polarite, zvyagintsevite, Pd-rich tetra-  
89 auricupride, Pd-Pt bearing auricupride, Ag-Au alloys, (Pb,As,Sb) bearing atokite, mayakite,  
90 Bi-Pb rich kotulskite and sperrylite in pentlandite, cubanite and talnakhite. The image of  
91 norilskite (No 229) with associated minerals of the type material from the Mayak mine is  
92 shown in Fig. 1.

93 Norilskite is opaque with a metallic lustre and grey streak. The powder of synthetic  
94 norilskite is grey in colour. The mineral is brittle. Values of  $\text{VHN}_{20}$  measured from 9  
95 indentations is in the range from 296 to 342  $\text{kg/mm}^2$ , with a mean value of 310  $\text{kg/mm}^2$ ,  
96 which corresponds to a Mohs hardness of about 4. The density calculated on the basis of the  
97 empirical formula is 12.99  $\text{g/cm}^3$ . In plane-polarized reflected light, norilskite is orange-  
98 brownish pink, has moderate to strong bireflectance, strong from orange-pink ( $R_o$ ) to greyish  
99 orange-pink ( $R_e$ ) pleochroism, and strong anisotropy with rotation tints from dull yellow to  
100 dull blue in partially crossed polars. It exhibits no internal reflections.

101 Reflectance measurements were made in air relative to a WTiC standard on both natural  
 102 and synthetic norilskite using a J & M TIDAS diode array spectrometer attached to a Zeiss  
 103 Axiotron microscope. The results are tabulated (Table 1) and illustrated in Fig. 2. With  $R_o >$   
 104  $R_e$  norilskite is uniaxial negative.

105

### 106 **Chemical composition**

107

108 Chemical analyses were performed with a CAMECA SX-100 electron probe microanalyser  
 109 (EPMA) in wavelength-dispersive mode using an electron beam focussed to 1-2  $\mu\text{m}$ . Pure  
 110 elements were used as standards. Concentrations were quantified on the  $\text{Pd}L_\alpha$ ,  $\text{Ag}L_\alpha$ ,  $\text{Bi}M_\alpha$   
 111 and  $\text{Pb}M_\alpha$  (with overlap correction on  $\text{Ag}L_\alpha$  and  $\text{Bi}M_\alpha$ ) with an accelerating voltage of 15  
 112 keV, and a beam current of 10 nA on the Faraday cup. Other elements were below detection  
 113 limit.

114 The electron-microprobe results are given in Table 2. The analyses of three grains from the  
 115 Mayak mine, Talnakh deposit gave close compositions with slightly variable Pd:Ag ratio  
 116 (based on 4 Pb+Bi atoms):  $(\text{Pd}_{6.56}\text{Ag}_{0.42})_{\Sigma 7.01}(\text{Pb}_{3.97}\text{Bi}_{0.03})_{\Sigma 4.00}$  (No 229),  
 117  $(\text{Pd}_{6.47}\text{Ag}_{0.38})_{\Sigma 6.87}(\text{Pb}_{3.98}\text{Bi}_{0.02})_{\Sigma 4.00}$  (No 208),  $(\text{Pd}_{6.66}\text{Ag}_{0.37})_{\Sigma 7.06}(\text{Pb}_{3.97}\text{Bi}_{0.03})_{\Sigma 4.00}$  (No 136) with  
 118 the empirical formulae for the average analysis ( $n=16$ )  $(\text{Pd}_{6.56}\text{Ag}_{0.39})_{\Sigma 6.97}(\text{Pb}_{3.97}\text{Bi}_{0.03})_{\Sigma 4.00}$ . The  
 119 proposed simplified formulae for norilskite is  $(\text{Pd,Ag})_7\text{Pb}_4$  with  $Z = 6$ . The Table 2 also  
 120 shows alternative recalculations of empirical formulae of norilskite based one Pb+Bi atoms  
 121 per formulae unit ( $Z = 24$ ) and on 11 atoms per formulae unit ( $Z = 6$ ). Nevertheless in  
 122 accordance with the crystal structure investigations (see “*Structure description*” section) we  
 123 are favourable to  $(\text{Pd,Ag})_7\text{Pb}_4$  formulae based on 4 Pb+Bi atoms.

124

125

126 **Synthetic analogue**

127

128 Tiny intergrowths of norilskite with lamellae of polarite and other minerals listed above  
129 embedded in pentlandite prevented its extraction and isolation in an amount sufficient for the  
130 relevant crystallographic and structural investigations. Therefore these investigations were  
131 performed on the synthetic phase  $(\text{Pd}_{6.25}\text{Ag}_{0.56})_{\Sigma 6.81}\text{Pb}_{4.00}$ .

132 The synthetic phase  $(\text{Pd}_{6.25}\text{Ag}_{0.56})_{\Sigma 6.81}\text{Pb}_{4.00}$  was prepared in an evacuated and sealed silica-  
133 glass tube in a horizontal furnace in the Laboratory of Experimental Mineralogy of the Czech  
134 Geological Survey in Prague. To prevent loss of material to the vapour phase during the  
135 experiment, the free space in the tube was reduced by placing a closely fitting glass rod  
136 against the charge. The temperature was measured with Pt-PtRh thermocouples and is  
137 accurate to within  $\pm 3$  °C. A charge of about 200 mg was carefully weighed out from the  
138 native elements. We used, as starting chemicals silver powder (Aldrich Chem. Co., 99.999%  
139 purity), lead ingot (Aldrich Chem. Co., 99.999% purity), and palladium powder (Aldrich  
140 Chem. Co., 99.95% purity). The starting mixture was first melted at 1000°C for two days. The  
141 product was then (from melting at 1000°C) ground in an agate mortar under acetone and  
142 reheated to 300°C for 113 days. The sample was quenched by dropping the capsule in cold  
143 water.

144

145 **X-ray crystallography**

146

147 A few grains of synthetic material were tested using single-crystal diffraction, however all  
148 crystals examined were found unsuitable for single-crystal analysis. Therefore, the crystal  
149 structure and unit cell parameters of synthetic norilskite were refined from the powder X-ray  
150 diffraction data.

151 The powder X-ray diffraction pattern used for the Rietveld refinement and refinement of  
152 lattice parameters was collected in Bragg-Brentano geometry on an X'Pert Pro PANalytical  
153 diffractometer, equipped with X'Celerator detector and a  $\text{CoK}\alpha$  radiation source. The data  
154 were collected in the range between 15 and  $135^\circ 2\theta$ . The details of data collection and basic  
155 crystallographic data are given in Table 3.

156 Inspection of the powder diffraction pattern of the synthetic analogue of norilskite  
157 indicated a positive match with the PDF-2 card no. 42-798 (ICDD 2002) denoted as the  
158  $\text{Pd}_6\text{AgPb}_4$  phase and the  $\text{Pd}_3\text{Pb}$  phase as a minor admixture (PDF-2 card no. 50-1631). The  
159 existence of a synthetic phase  $\text{Pd}_6\text{AgPb}_4$  is mentioned in the work of Sarah *et al.* (1981),  
160 where it is referred to as having the  $\text{Ni}_{13}\text{Ga}_3\text{Ge}_6$  structure type. However, neither crystal  
161 coordinates nor chemical data for the  $\text{Pd}_6\text{AgPb}_4$  phase have been published. The card no.  
162 605653 for the  $\text{Pd}_6\text{AgPb}_4$  phase, which can be found in the Inorganic Crystal Structure  
163 Database (ICSD 2015), contains the same structural data (i.e. atomic coordinates) as has the  
164 card no. 52177 for the  $\text{Ni}_{13}\text{Ga}_3\text{Ge}_6$  phase. Moreover, in the card 605653 is also a remark, that  
165 the coordinates were estimated by the database editor by the analogy to isotypic compounds.  
166 Therefore, the starting structure model of synthetic norilskite for subsequent Rietveld  
167 refinement was derived from the published data for the  $\text{Ni}_{13}\text{Ga}_3\text{Ge}_6$  phase (Nover and  
168 Schubert, 1981). In this structure model, the Ni atoms (8 independent positions) were  
169 substituted by the Pd atoms, the Ge atoms (3 independent positions) by the Pb atoms and the  
170 Ga atoms (2 independent positions) by the Ag atoms. This initial structure model of synthetic  
171 norilskite (Pd<sub>39</sub> Ag<sub>9</sub> Pb<sub>18</sub> atoms in the unit-cell) was refined by the Rietveld method for the  
172 powder X-ray diffraction data by means of the FullProf program (Rodríguez-Carvajal, 2006).  
173 The background was determined by the linear interpolation between consecutive breakpoints  
174 in the pattern. The refined parameters include those describing the peak shape and width, peak

175 asymmetry, unit cell parameters, fractional coordinates, occupancy parameters and an overall  
176 isotropic displacement parameter.

177 The occupancy parameters were carefully tested during the refinement (Pb against Pd, Ag  
178 against Pb), taking into account that it is not possible to distinguish between Ag and Pd atoms  
179 from conventional powder X-ray diffraction data (CoK $\alpha$  radiation). Consequently, the  
180 occupancy at the Ag(2) position (6c) was changed from Ag to Pb atoms, as was suggested by  
181 a significant drop of an  $R_{\text{Bragg}}$  factor (from 0.144 to 0.121) and a more reasonable coordination  
182 sphere for the other Ag atoms (octahedral coordination by Pb atoms). This substitution  
183 influences the chemical composition of the structure model. Whereas the former model  
184 contains Pd<sub>39</sub> Ag<sub>9</sub> Pb<sub>18</sub> atoms in the unit-cell, the new one has Pd<sub>39</sub> Ag<sub>3</sub> Pb<sub>24</sub> atoms in the  
185 unit-cell (result of Ag  $\rightarrow$  Pb substitution on position 6c). After recalculation for  $Z = 6$ , the  
186 structure-derived formula is (Pd<sub>6.50</sub>Ag<sub>0.50</sub>) $\Sigma$ <sub>7.00</sub>Pb<sub>4.00</sub>, which is in a very good agreement with  
187 the chemical composition obtained from electron microprobe analysis of the synthetic phase  
188 (Pd<sub>6.25</sub>Ag<sub>0.56</sub>) $\Sigma$ <sub>6.81</sub>Pb<sub>4.00</sub>.

189 The final cycles of refinement converged to the residual factors:  $R_{\text{Bragg}} = 0.098$ ,  $R_{\text{wp}} =$   
190  $0.045$  and  $R_{\text{p}} = 0.034$ . The crystal structure data are presented in Table 4, Fig. 3 shows the  
191 Rietveld plot. The crystal structure is depicted in Fig. 4 and 5, respectively. Since it is not  
192 possible to differentiate between Ag and Pd atoms in refinement from conventional powder  
193 X-ray diffraction data, all non-Pb positions are denoted as M1-M9. Table 5 presents an  
194 indexed powder-diffraction pattern of norilskite.

195

## 196 **Structure description**

197

198 The norilskite crystal structure can be viewed as a superstructure of the partially filled  
199 nickeline (NiAs) structure with doubled  $a$  and tripled  $c$  lattice parameters relative to the basic



200 unit-cell of the nickeline structure. In this basic structure, the As atoms form a hexagonal  
201 close packed (hcp) arrangement and Ni atoms occupy the octahedral interstices. Such  
202 structure contains also trigonal-bipyramidal voids. If all of these voids are occupied, one  
203 arrives at the Ni<sub>2</sub>In structure type. In the norilskite crystal structure, the Pb atoms show a  
204 distorted hexagonal close packing and all octahedral voids are occupied by M atoms (more  
205 specifically by M1, M2, M3, M4, M8 and M9 positions). Stoichiometry of such hypothetical  
206 compound is MPb and its crystal structure has the NiAs structure topology. However, 75 %  
207 of available trigonal-bipyramidal voids are occupied by additional M atoms (M5, M6, M7  
208 positions) in the norilskite crystal structure. This partial occupation results in (Pd+Ag)/Pb =  
209 1.75 ratio which corresponds very well with such ratio 1.70 obtained from electron  
210 microprobe analysis of synthetic material.

211 The partial occupation of trigonal-bipyramidal voids in norilskite implies short interatomic  
212 distances between M and Pb atoms, by comparison with the Pd-Pb distances observed in  
213 zvyagintsevite (2.85 Å; Ellner, 1981) and the PdPb<sub>2</sub> phase (2.95 Å; Havinga, 1972 ). The  
214 shortest interatomic contacts observed in the norilskite structure are 2.66 Å and 2.69 Å for  
215 M(7)-Pb(5) and M(5)-Pb(5) bonds, respectively. However, similar short metal-metal contacts  
216 were reported for the fully occupied Ni<sub>2</sub>In compound (Bhattacharya and Masson, 1976), so  
217 there seems to be no way to avoid such short interatomic distances in these compounds. On  
218 the other hand, partial occupancy of the trigonal bipyramidal voids might be a way to help the  
219 structure to relax (Norén *et al.*, 2000). The presence of vacancies seems to be an important  
220 stabilizing factor for the crystal structure of norilskite.

221 The alternative formulae of norilskite (Pd,Ag)<sub>1.70</sub>Pb<sub>1.00</sub> based on one Pb atom per formula  
222 unit ( $Z = 24$ ) clearly indicates its structural relationship with the NiAs and Ni<sub>2</sub>In structures. It  
223 also shows a proportion of trigonal-bipyramidal voids, which are occupied by Ag and Pd  
224 atoms (i.e. 75% of available voids). However, we have decided for (Pd,Ag)<sub>7</sub>Pb<sub>4</sub> ideal

225 formulae ( $Z = 6$ ), which reflects the fact that norilskite is an ordered superstructure relative to  
226 the NiAs and Ni<sub>2</sub>In structures. The presentation with Pd<sub>6</sub>(Pd,Ag)Pb<sub>4,00</sub> formulae can also be  
227 considered as another alternative. Nevertheless, since we were not able to reveal a distinct Ag  
228 site from conventional X-ray diffraction data, we prefer the (Pd,Ag)<sub>7</sub>Pb<sub>4</sub> ideal formulae for  
229 norilskite. The EMPA data of natural sample are also supportive for the (Pd,Ag)<sub>7</sub>Pb<sub>4</sub> ideal  
230 formulae (Table 2).

231

### 232 **Proof of identity of natural and synthetic norilskite**

233

234 The structural identity between the synthetic (Pd,Ag)<sub>7</sub>Pb<sub>4</sub> and the natural material was  
235 confirmed by electron back-scattering diffraction (EBSD). For that purpose, we used a  
236 TESCAN Mira 3GMU scanning electron microscope combined with EBSD system  
237 (NordlysNano detector, Oxford Instruments). The natural sample was prepared for  
238 investigation by the re-polishing the surface with colloidal silica (OP-U) for 5 minutes to  
239 reduce the surface damage. The EBSD patterns were collected and processed using a  
240 proprietary computer program AZtec HKL (Oxford Instruments). The solid angles calculated  
241 from the patterns were compared with a synthetic (Pd,Ag)<sub>7</sub>Pb<sub>4</sub> match containing 100  
242 reflectors to index the patterns. The Kikuchi patterns obtained from the natural material  
243 (seven measurements on different spots on natural norilskite) were found to match the  
244 patterns generated from the structure of synthetic (Pd,Ag)<sub>7</sub>Pb<sub>4</sub> provided by our crystal  
245 structure determination (Fig. 6). The values of the mean angular deviation (MAD goodness-  
246 of-fit in the solution) between the calculated and measured Kikuchi bands range between  
247 0.58° and 0.39°. These values reveal a very good match; mean angular deviations <1° are  
248 considered as indicators of an acceptable fit.

249 The EBSD study, chemical identity and optical properties confirmed the correspondence  
250 between natural and synthetic materials and thereby legitimise the use of the synthetic phase  
251 for the complete characterization of norilskite.

252

### 253 **Acknowledgements**

254

255 The authors acknowledge Ulf Hålenius, Chairman of the CNMNC and its members for  
256 helpful comments on the submitted data. They also acknowledge the helpful comments of  
257 Louis J. Cabri and an anonymous reviewer. The authors are grateful to Patricie Halodová and  
258 Jakub Haloda for carrying out the EBSD measurements. This work was supported by the  
259 internal project No. 337800 from the Czech Geological Survey.

260

### 261 **References**

262

263 Bhattacharya, B., Masson, D.B. (1976): Composition dependence of the thermodynamic  
264 activity and lattice parameter of eta nickel-indium, *Material Science and Engineering*  
265 **22**(5), 133-140.

266 Czamanske, G.K., Kunilov, V.Y., Zientek, M.L., Cabri, L.J., Likhachev A. P., Calk, L.C.,  
267 Oscarson, R.L. (1992) A proton-microprobe study of magmatic sulfide ores from the  
268 Noril'sk -Talnakh district, Siberia. *The Canadian Mineralogist*, **30**, 249-287.

269 Distler, V.V., Grokhovskaya, T.L., Evstigneeva, T.L., Sluzhenikin, S.F., Filimonova, A.A.,  
270 Dyuzhikov, O.A., Laputina, I.P. (1988) *Petrology of the sulphide magmatic*  
271 *mineralization*. Nauka, Moscow, pp 232 [in Russian].

- 272 Ellner, M. (1981): Zusammenhang zwischen strukturellen und thermodynamischen  
273 Eigenschaften bei Phasen der Kupferfamilie in  $T_{10}B_4$  – Systemen. *Journal of Less*  
274 *Common Metals*, **78**, 21-32.
- 275 Genkin, A.D. & Evstigneeva, T.L. (1986) Associations of platinum-group minerals of the  
276 Noril'sk copper-nickel sulphide ores. *Economic Geology*, **81**, 1203-1212.
- 277 Genkin, A.D. (1968) Minerals of the platinum metals and their associations in the copper-  
278 nickel ores of the Noril'sk deposits. Nauka, pp 106 [in Russian].
- 279 Genkin, A.D., Distler, V.V., Gladyshev, G.D., Filimonova, A.A., Evstigneeva, T.L.,  
280 Kovalenker, V.A., Laputina, I.P., Smirnov, A.B., Grokhovskaya, T.L. (1981) *Sulphide*  
281 *nickel-copper ores of the Noril'sk deposits*. Nauka, Moscow, pp 234 [in Russian].
- 282 Havinga, E.E., Damsma, H., Hokkeling, P. (1972): Compounds and pseudo-binary alloys with  
283 the  $CuAl_2$  (C16)-type structure. I. Preparation and X-ray results. *Journal of Less Common*  
284 *Metals*, **27**, 169-186.
- 285 ICDD (2002): Powder diffraction file, International Centre for Diffraction Data, edited by  
286 Frank McClune, 12 Campus Boulevard, Newton Square, PA 19073-3272, USA.
- 287 Inorganic Crystal Structure Database (2015): Fachinformationszentrum Karlsruhe (Germany)  
288 and National Institute of Standards and Technology (Maryland, USA).
- 289 Komarova, M.Z., Kozyrev, S.M., Simonov, O.N., Lulko, V.A. (2002) The PGE  
290 mineralization of disseminated sulphide ores of the Noril'sk -Taimyr region. In: Cabri,  
291 L.J. (ed.) *The Geology, Geochemistry, Mineralogy and Mineral Beneficiation of*  
292 *Platinum-Group Elements*, CIM Special Vol. 54, 547-567.
- 293 Naldrett, A.J., Lightfoot, P.C., Fedorenko, V., Doherty, W. & Gorbachev, N.S. (1992):  
294 Geology and Geochemistry of Intrusions and Flood Basalts of the Noril'sk Region,  
295 USSR, with Implications for the Origin of the Ni-Cu Ores. *Economic Geology*, **87**, 975-  
296 1004.

- 297 Norén, L., Withers, R.L., Tabira, Y. (2000) New B8<sub>1</sub> – B8<sub>2</sub> phases in the Ni – In system.  
298 *Journal of Alloys Compounds*, **309**, 179-187.
- 299 Nover, G. and Schubert, K. (1981): Crystal Structure of Ni<sub>13</sub>Ga<sub>3</sub>Ge<sub>6</sub>. *Zeitschrift für*  
300 *Metallkunde*, **72**, 26-29.
- 301 Rodríguez-Carvajal, J. (2006): FullProf.2k Rietveld Profile Matching & Integrated Intensities  
302 Refinement of X-ray and/or Neutron Data (powder and/or single-crystal). Laboratoire  
303 Léon Brillouin, Centre d'Études de Saclay, Gif-sur-Yvette Cedex, France.
- 304 Sarah, N., Alasafi, K., Schubert, K. (1981): Kristallstruktur von Pd<sub>20</sub>Sn<sub>13</sub>, Pd<sub>6</sub>AgPb<sub>4</sub> und  
305 Ni<sub>13</sub>ZnGe<sub>8</sub>. *Zeitschrift für Metallkunde*, **72**(7), 517-520.
- 306 Sluzhenikin, S.F. and Mokhov, A.V. (2015): Gold and silver in PGE-Cu-Ni and PGE pres of  
307 the Noril'sk deposit, Russia. *Mineralium Deposita*, **50**, 465-492.
- 308 Sluzhinikin, S.F. (2011) Platinum-copper-nickel and platinum ores of Noril'sk region and  
309 their ore mineralization. *Russian Journal of General Chemistry*, **81**(6), 1288-1301.
- 310 Zviaginцев, O.E. (1940) New mineral species of the platinum group. *Doklady Akademii Nauk*  
311 *SSSR*, **26**, 8, 788-791.
- 312
- 313
- 314
- 315
- 316
- 317
- 318
- 319
- 320
- 321

322 TABLES

323

324 TABLE 1. Reflectance data for norilskite

325

326 TABLE 2. Electron-microprobe analyses of natural and synthetic norilskite and three  
327 recalculations of norilskite stoichiometry (based on Pb+Bi = 4 apfu, Pb+Bi = 1 apfu, and 11  
328 apfu).

329

330 TABLE 3. Powder X-ray diffraction experimental details and Rietveld analysis of norilskite

331

332 TABLE 4. Atomic positions for synthetic norilskite (space group  $P3_121$ ,  $B_{\text{iso(overall)}} = 0.12(2)$   
333  $\text{\AA}^2$ ), M(1)-M(7) represent Pd or/and Ag atoms.

334

335 TABLE 5. X-ray powder-diffraction data for synthetic norilskite (CoK $\alpha$  radiation). Reflections  
336 with intensities  $\geq 1\%$  are shown.

337

338 FIGURES

339

340 FIG. 1. Images of norilskite (nor) from the type locality Mayak mine of the Talnakh deposit,  
341 Noril'sk district (Sample No 229) and associated minerals (a) Back-scattered electron (BSE)  
342 image (b) reflected light photomicrograph of the same grain, zvyagintsevite (zvy),  
343 auricupride (aur), tetra-auricupride (tet), polarite (pol) and Ag-Au alloys.

344

345 FIG. 2. Reflectance data for natural norilskite compared to synthetic in air. The reflectance  
346 values (R %) are plotted versus wavelength  $\lambda$  in nm.

347

348 FIG. 3. Observed (circles), calculated (solid lines) and difference Rietveld profiles for  
349 norilskite. The upper reflection markers correspond to norilskite and the lower markers to a  
350 Pd<sub>3</sub>Pb (7 wt. %) impurity.

351

352 FIG. 4. Polyhedral representation of (a, b) the norilskite crystal structure showing the [MPb<sub>6</sub>]  
353 distorted octahedra (M = Pd or Ag) and (c) the NiAs (nickeline) structure. Unit-cell edges are  
354 highlighted.

355

356 FIG. 5. (a) View along the *c* axis showing a layer composed of [MPb<sub>6</sub>] edge-sharing  
357 octahedra (green) and trigonal-bipyramidal sites (brown) occupied by additional M atoms  
358 (M=Pd,Ag), (b) detailed view of the trigonal-bipyramidal site.

359

360 FIG. 6. EBSD image of natural norilskite; in the right pane, the Kikuchi bands are indexed.

361

362

TABLE 1. Reflectance data for natural and synthetic norilskite.

$\lambda$ (nm)	natural		synthetic	
	Ro (%)	Re' (%)	Ro (%)	Re' (%)
400	46.6	44.9	47.1	45.1
420	47.9	45.9	48.4	46.1
440	49.0	46.9	49.6	47.3
460	50.4	48.2	51.1	48.7
<b>470</b>	<b>51.1</b>	<b>48.8</b>	<b>51.8</b>	<b>49.4</b>
480	51.8	49.4	52.5	50.0
500	53.3	50.4	53.9	51.2
520	54.7	51.2	55.3	52.2
540	56.3	52.0	56.7	53.2
<b>546</b>	<b>56.8</b>	<b>52.2</b>	<b>57.1</b>	<b>53.5</b>
560	57.9	52.5	58.1	54.1
580	59.7	53.1	59.6	54.9
<b>589</b>	<b>59.9</b>	<b>53.5</b>	<b>59.9</b>	<b>55.2</b>
600	61.1	53.8	61.2	55.6
620	62.7	54.4	62.3	56.5
640	64.0	55.1	63.9	57.2
<b>650</b>	<b>64.7</b>	<b>55.5</b>	<b>64.4</b>	<b>57.7</b>
660	65.4	55.8	65.0	58.1
680	66.6	57.0	66.4	59.0
700	67.8	58.1	67.5	60.0

Note: The values required by the Commission on Ore Mineralogy are given in bold.



TABLE 2. Electron-microprobe analyses of natural and synthetic norilskite and three recalculations of norilskite stoichiometry (based on Pb+Bi = 4 apfu, Pb+Bi = 1 apfu, and 11 apfu).

Natural sample						(Pd,Ag) <sub>7</sub> Pb <sub>4</sub> (Z=6)			(Pd,Ag) <sub>2-x</sub> Pb (Z=24)			(Pd,Ag) <sub>7</sub> Pb <sub>4</sub> (Z=6)			
No	Pd	Ag	Pb	Bi	Total	Pb=4			Pb=1			apfu 11			
	wt. %					Pd	Ag	Pb+Bi	Pd	Ag	Pb+Bi	Pd	Ag	Pb	Bi
229 (2)	45.01	2.91	52.30	0.44	100.66	6.65	0.42	4.00	1.66	0.11	1.00	6.60	0.42	3.94	0.03
229 (2)	44.39	3.20	52.42	0.32	100.34	6.56	0.47	4.00	1.64	0.12	1.00	6.54	0.46	3.97	0.02
229 (2)	44.65	2.78	52.71	0.39	100.53	6.55	0.40	4.00	1.64	0.10	1.00	6.58	0.40	3.99	0.03
229 (2)	44.02	2.84	52.35	0.43	99.63	6.50	0.41	4.00	1.62	0.10	1.00	6.55	0.42	4.00	0.03
229 (2)	44.80	2.85	53.07	0.36	101.07	6.53	0.41	4.00	1.63	0.10	1.00	6.57	0.41	3.99	0.03
avg (n=5)	44.57	2.91	52.57	0.39	100.44	6.56	0.42	4.00	1.64	0.11	1.00	6.57	0.42	3.98	0.03
208	44.84	2.88	52.94	0.25	100.91	6.57	0.42	4.00	1.64	0.10	1.00	6.58	0.42	3.99	0.02
208	43.56	2.60	52.62	0.19	98.97	6.43	0.38	4.00	1.61	0.09	1.00	6.54	0.39	4.06	0.01
208	44.21	2.52	52.47	0.34	99.54	6.52	0.37	4.00	1.63	0.09	1.00	6.59	0.37	4.02	0.03
208	44.35	2.52	53.09	0.35	100.31	6.46	0.36	4.00	1.62	0.09	1.00	6.57	0.37	4.04	0.03
208	43.64	2.76	53.14	0.25	99.80	6.37	0.40	4.00	1.59	0.10	1.00	6.51	0.41	4.07	0.02
208	44.59	2.48	53.21	0.29	100.57	6.49	0.36	4.00	1.62	0.09	1.00	6.58	0.36	4.03	0.02
avg (n=6)	44.20	2.63	52.91	0.28	100.02	6.47	0.38	4.00	1.62	0.09	1.00	6.56	0.38	4.03	0.02
136-2	44.25	2.31	51.23	0.12	97.91	6.71	0.35	4.00	1.68	0.09	1.00	6.68	0.34	3.97	0.01
136-2	44.04	2.39	50.53	0.45	97.41	6.73	0.36	4.00	1.68	0.09	1.00	6.68	0.36	3.93	0.04
136-2	44.09	2.46	52.06	0.31	98.92	6.56	0.36	4.00	1.64	0.09	1.00	6.61	0.36	4.01	0.02
136-2	44.73	2.61	51.68	0.49	99.51	6.68	0.38	4.00	1.67	0.10	1.00	6.64	0.38	3.94	0.04
136-2	44.12	2.82	51.57	0.35	98.86	6.62	0.42	4.00	1.65	0.10	1.00	6.60	0.42	3.96	0.03
avg (n=5)	44.24	2.52	51.41	0.35	98.52	6.66	0.37	4.00	1.66	0.09	1.00	6.64	0.37	3.96	0.03
avg (n=15)	44.33	2.68	52.34	0.33	99.68	6.56	0.39	4.00	1.64	0.10	1.00	6.59	0.39	3.99	0.03
Std. dev.	0.39	0.22	0.72	0.09											

Synthetic sample					(Pd,Ag) <sub>7</sub> Pb <sub>4</sub> (Z=6)			(Pd,Ag) <sub>2-x</sub> Pb (Z=24)			(Pd,Ag) <sub>7</sub> Pb <sub>4</sub> (Z=6)		
	Pd	Ag	Pb	Total	Pb=4			Pb=1			apfu 11		
	wt.%				Pd	Ag	Pb	Pd	Ag	Pb	Pd	Ag	Pb
Exp33	43.28	3.64	53.94	100.85	6.25	0.52	4.00	1.56	0.13	1.00	6.38	0.53	4.09
Exp33	42.63	4.34	53.07	100.03	6.26	0.63	4.00	1.56	0.16	1.00	6.32	0.63	4.04
Exp33	42.21	4.18	53.48	99.87	6.15	0.60	4.00	1.54	0.15	1.00	6.29	0.61	4.09
Exp33	43.19	3.63	53.67	100.50	6.27	0.52	4.00	1.57	0.13	1.00	6.39	0.53	4.08
Exp33	42.88	4.66	53.09	100.63	6.29	0.67	4.00	1.57	0.17	1.00	6.31	0.68	4.01
Exp33	42.80	3.43	53.25	99.48	6.26	0.49	4.00	1.57	0.12	1.00	6.40	0.51	4.09
Exp33	42.88	3.92	53.71	100.50	6.22	0.56	4.00	1.55	0.14	1.00	6.35	0.57	4.08
Exp33	43.72	3.19	53.89	100.79	6.32	0.45	4.00	1.58	0.11	1.00	6.45	0.46	4.08
avg ( <i>n</i> =8)	42.95	3.87	53.51	100.33	6.25	0.56	4.00	1.56	0.14	1.00	6.36	0.57	4.07
Std. dev.	0.42	0.46	0.32	0.45									

TABLE 3. Powder X-ray diffraction experimental details and Rietveld analysis of norilskite

---

Data collection	
Radiation type, source	X-ray, CoK $\alpha$
Generator settings	40kV, 30mA
Range in $2\theta$ ( $^\circ$ )	15 -135
Step size ( $^\circ$ )	0.02
Crystal data	
Space group	$P3_121$
Unit-cell content	$Z = 6$
Unit-cell parameters ( $\text{\AA}$ )	$a = 8.9656(4)$ $c = 17.2801(8)$
Unit-cell volume ( $\text{\AA}^3$ )	1202.92(9)
Rietveld analysis	
No. of reflections	531
No. of structural parameters	31
No. of profile parameters	4
$R_{\text{Bragg}}$	0.098
$R_p$	0.034
$R_{\text{wp}}$	0.045
Weighting scheme	$1/y_o$

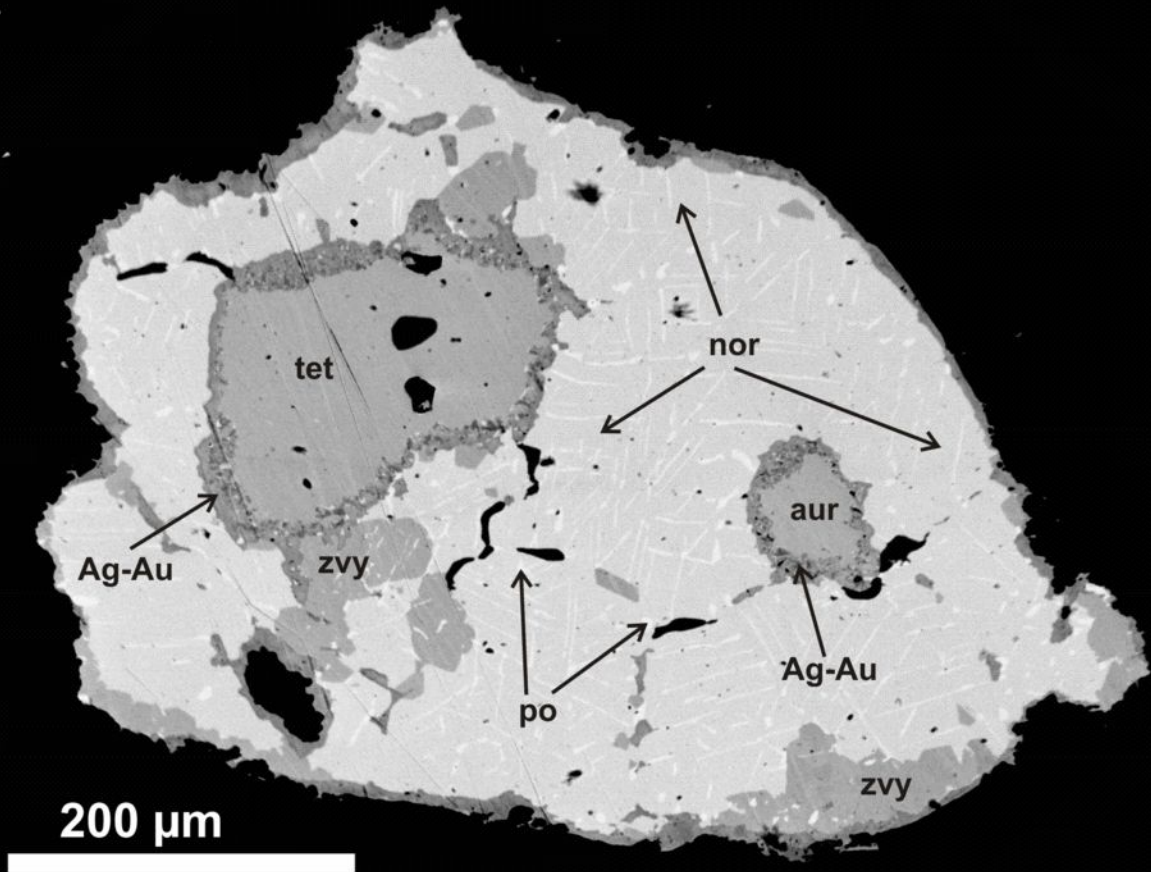
---

TABLE 4. Atomic positions for synthetic norilskite (space group  $P3_121$ ,  $B_{\text{iso(overall)}} = 0.12(2)$  Å<sup>2</sup>), M(1)-M(7) represent Pd or/and Ag atoms.

Atom	Wyckoff letter	$x$	$y$	$z$
M(1)	$3a$	0.492(5)	0	1/3
M(2)	$3b$	0.996(6)	0	5/6
M(3)	$6c$	0.998(7)	0.503(5)	0.3213(9)
M(4)	$6c$	0.507(5)	0.006(5)	0.162(1)
M(5)	$6c$	0.315(4)	0.658(3)	0.0930(9)
M(6)	$6c$	0.333(4)	0.178(4)	0.420(1)
M(7)	$6c$	0.153(3)	0.343(4)	0.259(1)
M(8)	$3a$	0.012(4)	0	1/3
M(9)	$3b$	0.497(7)	0	5/6
Pb(1)	$6c$	0.184(4)	0.309(4)	0.0839(6)
Pb(2)	$6c$	0.623(2)	0.305(2)	0.0852(7)
Pb(3)	$6c$	0.340(2)	0.169(2)	0.2545(5)
Pb(4)	$6c$	0.123(1)	0.316(3)	0.4129(7)

TABLE 5. X-ray powder-diffraction data for synthetic norilskite (CoK $\alpha$  radiation). Reflections with intensities  $\geq 1\%$  are shown.

<i>h</i>	<i>k</i>	<i>l</i>		<i>I</i> <sub>(obs)</sub>	<i>I</i> <sub>(calc)</sub>	<i>d</i> <sub>(obs)</sub>	<i>d</i> <sub>(calc)</sub>
0	2	3	}	29	13	3.2201	3.2192
2	0	3					3.2192
1	2	1		8	7	2.8905	2.8932
0	0	6		11	13	2.8819	2.8801
1	2	2		7	6	2.7788	2.7787
0	3	1		4	4	2.5584	2.5595
0	3	2	}	8	2	2.4790	2.4792
3	0	2					2.4792
1	2	4	}	6	1	2.4274	2.4275
2	1	4					2.4275
0	2	6	}	91	59	2.3130	2.3131
2	0	6					2.3131
2	2	0		100	100	2.2414	2.2413
1	2	7		2	3	1.8886	1.8891
0	4	3	}	6	3	1.8396	1.8394
4	0	3					1.8394
2	2	6		13	15	1.7690	1.7688
0	2	9	}	6	4	1.7212	1.7211
2	0	9					1.7211
1	4	2	}	4	2	1.6626	1.6626
4	1	2					1.6626
0	4	6	}	28	12	1.6098	1.6096
4	0	6					1.6096
5	0	1		3	3	1.5467	1.5466
0	0	12		11	11	1.4402	1.4401
1	5	2	}	3	2	1.3767	1.3767
5	1	2					1.3767
5	1	4		2	2	1.3271	1.3271
2	4	6	}	38	23	1.3076	1.3074
4	6	2					1.3074
6	0	0		18	18	1.2942	1.2941
2	5	2		3	3	1.2307	1.2306
2	2	12	}	37	36	1.2115	1.2115
1	2	13					1.2108
2	5	4	}	4	3	1.1950	1.1948
5	2	4					1.1948
4	4	0		11	11	1.1208	1.1207
5	2	8		4	3	1.0776	1.0776
2	6	6	}	15	5	1.0086	1.0085
6	2	6					1.0085
0	6	12	}	44	20	0.9626	0.9625
6	0	12					0.9625

**A**

**B**

cpy

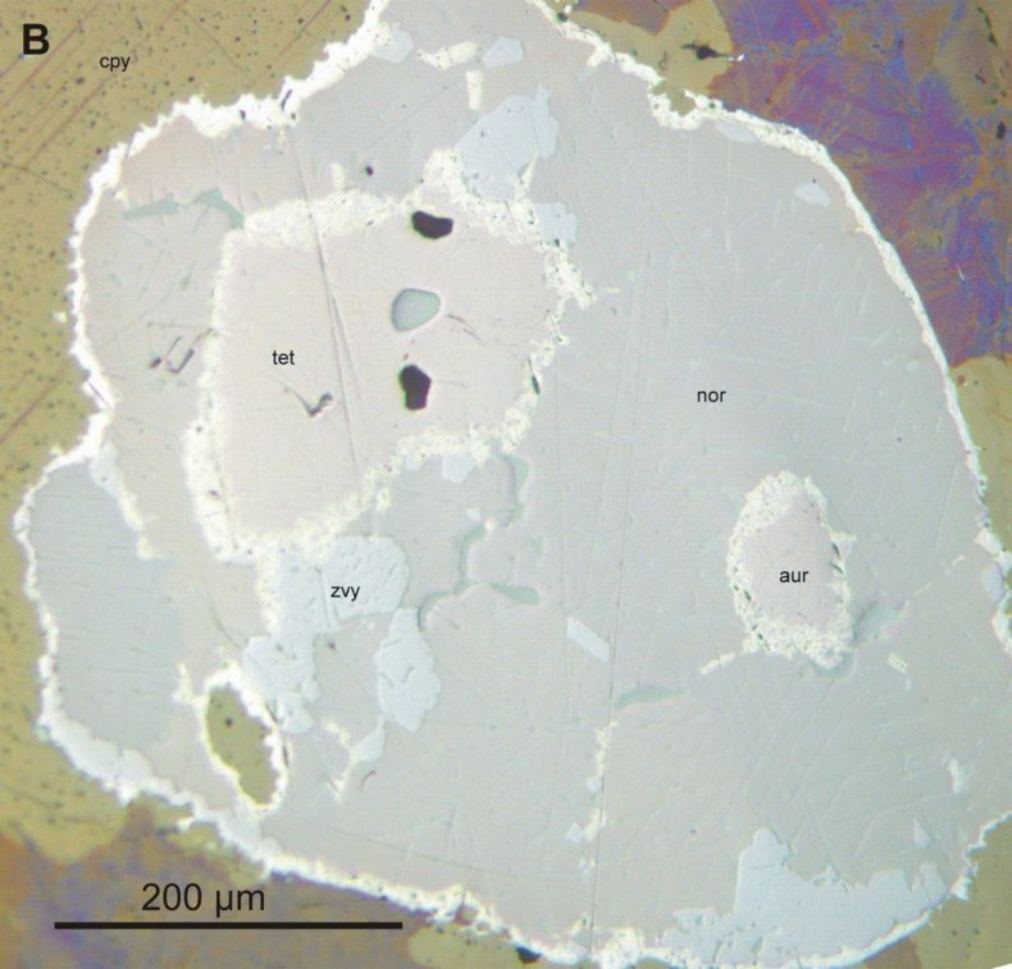
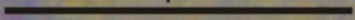
tet

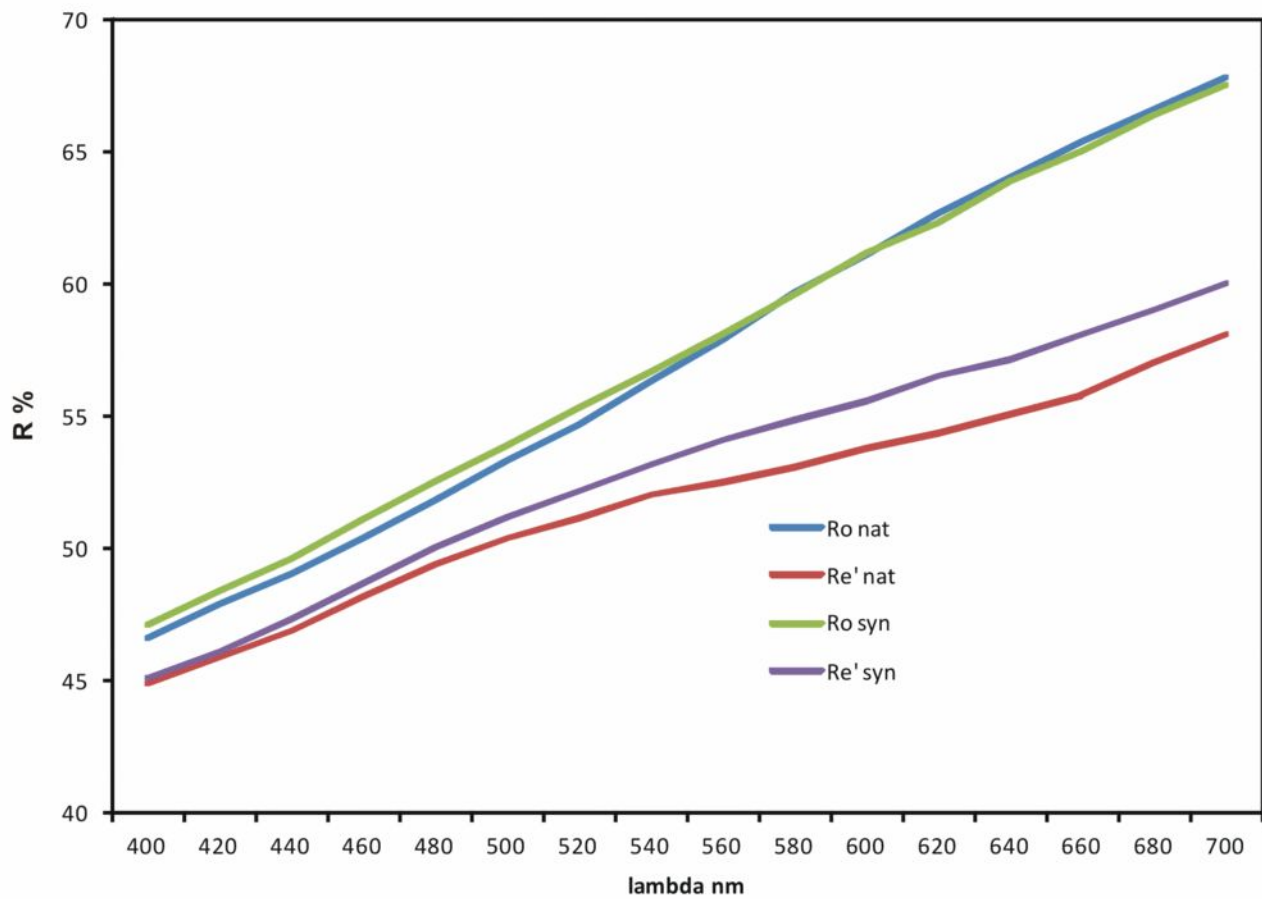
nor

zvy

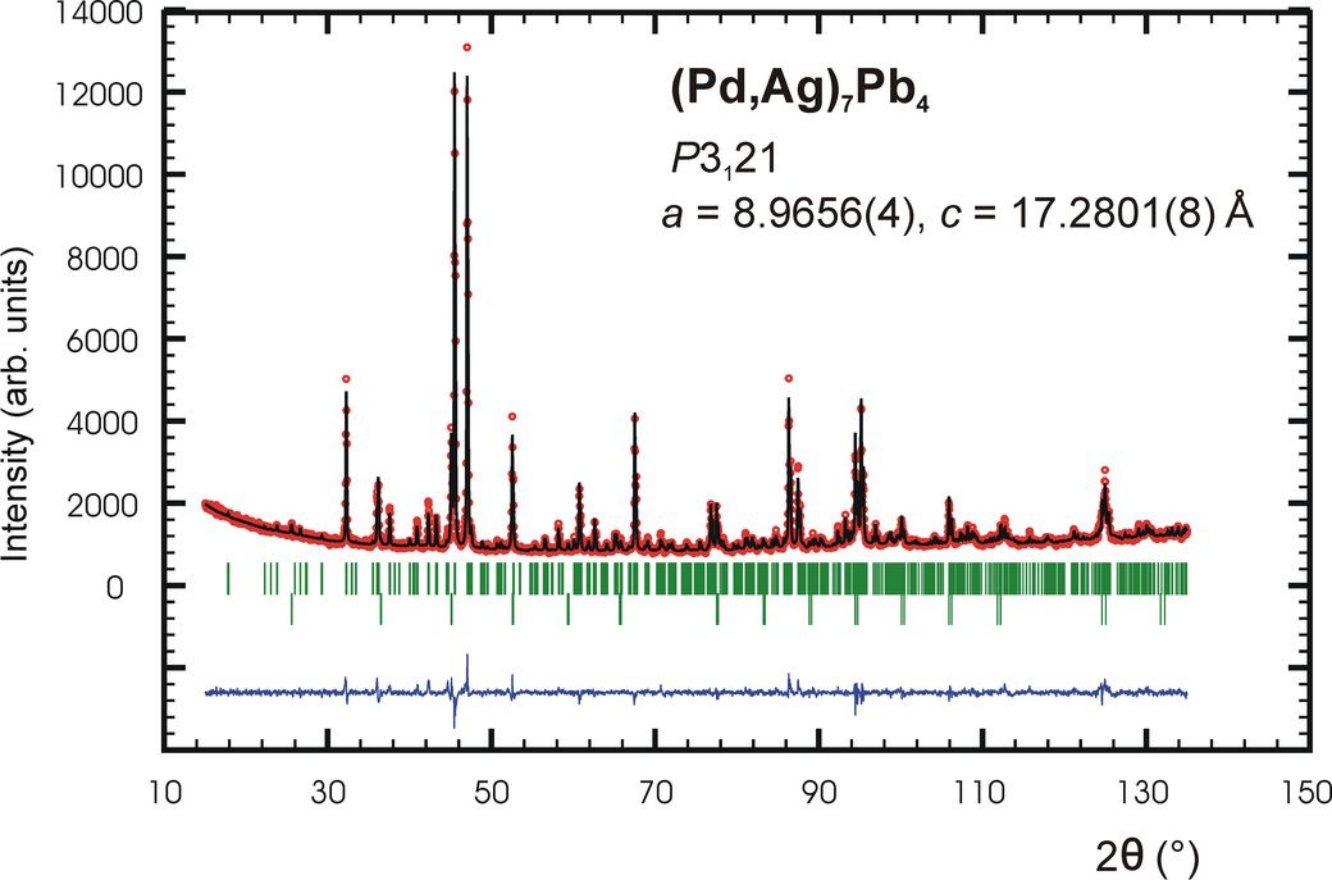
aur

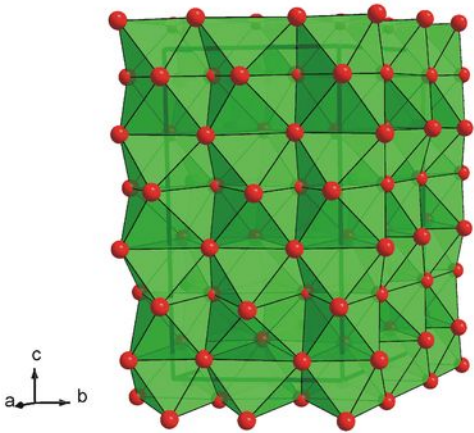
200  $\mu$ m



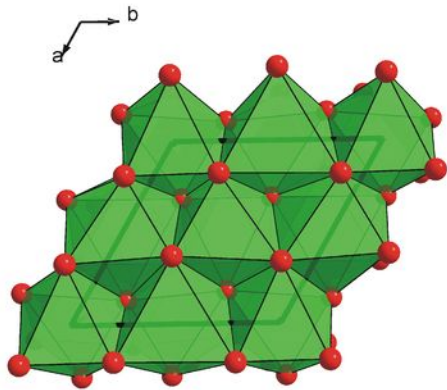




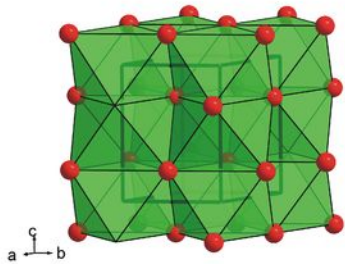




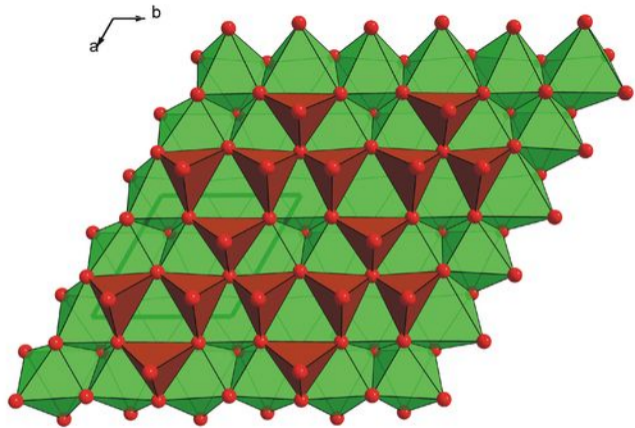
(a)



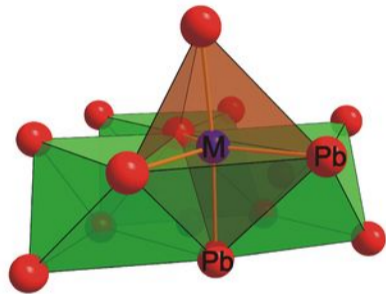
(b)



(c)



(a)



(b)

